

Evidence for a subcortical origin of mirror movements after stroke: a longitudinal study

Naveed Ejaz,^{1,*} Jing Xu,^{2,*} Meret Branscheidt,^{3,4} Benjamin Hertler,³ Heidi Schambra,⁵ Mario Widmer,^{3,6} Andreia V. Faria,⁷ Michelle D. Harran,² Juan C. Cortes,² Nathan Kim,² Pablo A. Celnik,⁴ Tomoko Kitago,⁸ Andreas R. Luft,^{3,6} John W. Krakauer^{2,4} and Jörn Diedrichsen¹

*These authors contributed equally to this work.

Following a stroke, mirror movements are unintended movements that appear in the non-paretic hand when the paretic hand voluntarily moves. Mirror movements have previously been linked to overactivation of sensorimotor areas in the non-lesioned hemisphere. In this study, we hypothesized that mirror movements might instead have a subcortical origin, and are the by-product of subcortical motor pathways upregulating their contributions to the paretic hand. To test this idea, we first characterized the time course of mirroring in 53 first-time stroke patients, and compared it to the time course of activities in sensorimotor areas of the lesioned and non-lesioned hemispheres (measured using functional MRI). Mirroring in the non-paretic hand was exaggerated early after stroke (Week 2), but progressively diminished over the year with a time course that paralleled individuation deficits in the paretic hand. We found no evidence of cortical overactivation that could explain the time course changes in behaviour, contrary to the cortical model of mirroring. Consistent with a subcortical origin of mirroring, we predicted that subcortical contributions should broadly recruit fingers in the non-paretic hand, reflecting the limited capacity of subcortical pathways in providing individuated finger control. We therefore characterized finger recruitment patterns in the non-paretic hand during mirroring. During mirroring, non-paretic fingers were broadly recruited, with mirrored forces in homologous fingers being only slightly larger (1.76 times) than those in non-homologous fingers. Throughout recovery, the pattern of finger recruitment during mirroring for patients looked like a scaled version of the corresponding control mirroring pattern, suggesting that the system that is responsible for mirroring in controls is upregulated after stroke. Together, our results suggest that post-stroke mirror movements in the non-paretic hand, like enslaved movements in the paretic hand, are caused by the upregulation of a bilaterally organized subcortical system.

- 1 Brain and Mind Institute, Western University, London, Canada
- 2 Department of Neurology, Neuroscience, Johns Hopkins University, Baltimore, USA
- 3 Department of Neurology, University of Zurich, Zurich, Switzerland
- 4 Department of Physical Medicine and Rehabilitation, Johns Hopkins University, Baltimore, USA
- 5 Department of Neurology, New York University, New York, USA
- 6 Cereneo Center for Neurology and Rehabilitation, Vitznau, Switzerland
- 7 Department of Radiology, Johns Hopkins University, Baltimore, USA
- 8 Burke Medical Research Institute, Weill Cornell Medicine, New York, USA

Correspondence to: Naveed Ejaz
Brain and Mind Institute, Western University, London, Canada
E-mail: nejaz2@uwo.ca

Keywords: mirror movements; stroke; recovery; corticospinal; reticulospinal

Abbreviation: BOLD = blood oxygen level-dependent; S1 = primary somatosensory cortex; M1 = primary motor cortex

Received April 21, 2017. Revised November 17, 2017. Accepted November 23, 2017.

© The Author(s) (2018). Published by Oxford University Press on behalf of the Guarantors of Brain. All rights reserved.

For Permissions, please email: journals.permissions@oup.com

Introduction

Mirror movements are unintended movements that appear in the passive hand when the active hand voluntarily moves. Even healthy individuals show low levels of mirror movements, which increase proportionally with the applied force level (Todor and Lazarus, 1986; Armatas *et al.*, 1996). Mirroring is especially prominent after stroke, with patients' attempts to move their paretic hand often resulting in exaggerated involuntary movements in their non-paretic hand (Cernacek, 1961; Nelles *et al.*, 1998; Kim *et al.*, 2003, 2015). The occurrence and evolution over time of mirror movements provide a potential window into post-stroke reorganization of the motor system. Despite this potential importance, no work has carefully characterized the time course and pattern of mirror movements after stroke, and little is known about the phenomenon's locus of origin.

One possible cause for mirror movements is that they arise due to overactivation of the non-lesioned hemisphere after stroke (Cincotta and Ziemann, 2008). This overactivation could be maladaptive, or exist to provide compensatory control of the paretic hand (Di Pino *et al.*, 2014). Either way, activity in the non-lesioned sensorimotor areas would lead to mirror movements by activating the non-paretic hand via the crossed corticospinal tract. Consistent with this idea, functional MRI studies have reported increased activity in the non-lesioned sensorimotor cortex post-stroke (Cramer *et al.*, 1997; Wittenberg *et al.*, 2000; Kim *et al.*, 2003; Ward *et al.*, 2003).

Alternatively, post-stroke mirror movements could be caused by the activity of phylogenetically-older subcortical motor circuits that contribute to control. The importance of these subcortical pathways in hand function was clearly demonstrated by Lawrence and Kuypers (1968*a*) who performed bilateral interruptions of the pyramidal tracts. They showed that subcortical pathways originating in the brainstem (i.e. rubrospinal, reticulospinal) can provide the substrate for substantial recovery of hand function following corticospinal damage, even though their capacity for fine individuation of finger movements was limited. Given their limited ability for fine-fractionated control, a post-stroke upregulation in these subcortical pathways has been proposed to give rise to intrusive movements (synergies) in the paretic upper-limb (Sukal *et al.*, 2007; Lan *et al.*, 2017; Xu *et al.*, 2017). We propose that mirror movements could be similar intrusive movements in the non-paretic hand that also arise due to upregulated subcortical motor pathways post-stroke. Specifically, strong bilateral organization of these subcortical pathways make them ideally-suited to produce mirror movements: individual axons originating in the ponto-medullary reticular formation project bilaterally onto ipsi- (~60%) and contralateral (~40%) sections of the spinal cord (Sakai *et al.*, 2009), and activate upper-limb muscles on either side of the body (Hirschauer and Buford, 2015).

The aim of our study was therefore to determine whether post-stroke mirror movements in the non-paretic hand are generated cortically or subcortically. To do this, we provide a careful characterization of the year-long changes in mirror movements in 53 first-time stroke patients. We first compared the time course of non-paretic mirroring with the time course of non-lesioned sensorimotor activity measured with functional MRI. We predicted that if non-paretic mirroring was generated cortically, then larger degrees of mirroring should be associated with greater non-lesioned sensorimotor activity. We also quantified the pattern with which non-paretic fingers were recruited during individuated finger presses with the paretic hand. We hypothesized that a subcortical origin for mirroring should result in a broad recruitment of fingers in the passive hand, reflecting limited ability of brainstem pathways in providing individuated finger control (Lawrence and Kuypers, 1968*b*; Soteropoulos *et al.*, 2012). In contrast, we hypothesized that a trans-callosal origin for mirroring should primarily recruit the homologous finger in the non-paretic hand. We based this hypothesis on recent non-invasive imaging work (functional MRI; Diedrichsen *et al.*, 2013, 2017) and invasive recordings (electrocorticography; Scherer *et al.*, 2009; Liu *et al.*, 2010), which demonstrate that the cortical activity patterns for the ipsilateral hand are weaker versions, but otherwise identical to the patterns elicited by the mirror-symmetric movement on the contralateral hand. If mirror movements are caused by involuntary outflow of this cortical activity, the resulting forces produced should be (up to a scaling factor) exact mirror images of the forces produced by fingers in the active hand.

Materials and methods

Participants

Fifty-three patients with hemiparesis [20 female; mean age = 57.4, standard deviation (SD) = 14.9 years] were recruited within the first 2 weeks after stroke. The recovery of paretic hand function is reported in Xu *et al.* (2017), but clinical measures of impairment at the time of recruitment are summarized in [Supplementary Fig. 1](#). Patients were included if they had a first-time unilateral ischaemic stroke and reported unilateral weakness of the upper extremity (Medical Research Council muscle weakness scale < 5). They were excluded if aged < 21 years, their initial upper-limb impairment was too mild (Fugl-Meyer > 63/66), or if they had cognitive deficits that could impair task comprehension and performance. Patients with receptive aphasia were excluded to reduce the likelihood that impaired behavioural performance was due to the inability to comprehend task instructions. Excluding aphasic patients led to a bias of right-hemispheric infarcts (36 right), in turn leading to a disproportionately higher ratio of left-handed patients Goodglass and Quadfasel (1954) [11 left-hand according to Oldfield (1971), 20.8% of patients in the cohort were left-handed]. A comprehensive list of inclusion/exclusion criteria is available from Xu *et al.* (2017).

Fourteen neurologically-healthy participants were also recruited as healthy controls for the study (four female; mean

age = 64.0, SD = 8.2 years). Controls and patients did not differ in age [$t(65) = 1.60$, $P = 0.11$].

Data were collected across three centres: Johns Hopkins University, University of Zurich, and Columbia University. All experimental procedures were approved by the respective local ethics committee, and written consent was obtained from all participants.

Apparatus to measure finger forces

We used a custom-built ergonomic keyboard (Fig. 1A) to measure isometric finger forces generated during the behavioural and functional MRI tasks. During either experiment, participants were instructed to always keep both their hands on the 10 keys of the device. Force transducers beneath each key (Honeywell FS, dynamic range 0–25 N) allowed for the sensitive measurement of finger forces in the instructed hand (Ejaz *et al.*, 2015; Xu *et al.*, 2017) (Fig. 1B), as well as mirrored finger forces in the passive hand (Diedrichsen *et al.*, 2013).

Assessment of mirror movements during the behavioural task

Mirror movements for each participant (patients and controls) were assessed over five longitudinal measurement sessions following recruitment (Table 1); Weeks 2, 4, 12, 24 and 52 post-stroke.

During each measurement session, participants performed individuated force presses in the flexion direction with the

instructed finger, while mirrored forces in the fingers of the passive hand were recorded. A visual representation of all 10 fingers was presented on a screen (Fig. 1A). The experiment began by estimating the strength of each finger, measuring two repetitions of the maximum voluntary force of each digit on both hands.

All subsequent trials required the production of isometric fingertip forces at a fraction of the maximum voluntary force for the instructed digit (at 20%, 40%, 60%, 80%). At the start of every trial, a force target-zone (target-force \pm 25%) on a single finger was highlighted in green. This was the cue for participants to make a short force press with the instructed finger to match and maintain the target-force for 0.5 s while keeping the uninstructed fingers in either hand as motionless as possible. The trial was stopped if force on the instructed digit did not exceed 2.5 N in the 2 s following stimulus onset. Trials were presented in sequential order, starting from the left thumb to the left little finger, and ending with the right thumb to the right little finger. Trials were grouped as blocks, with each block consisting of one measurement each for the four target-force levels across the 10 fingers (four target-force levels \times 10 fingers = 40 trials/block). Participants performed four such blocks during each measurement session.

Quantifying the degree of mirror movements

During each trial, finger presses with the instructed finger resulted in subtle forces in the fingers of the passive hand

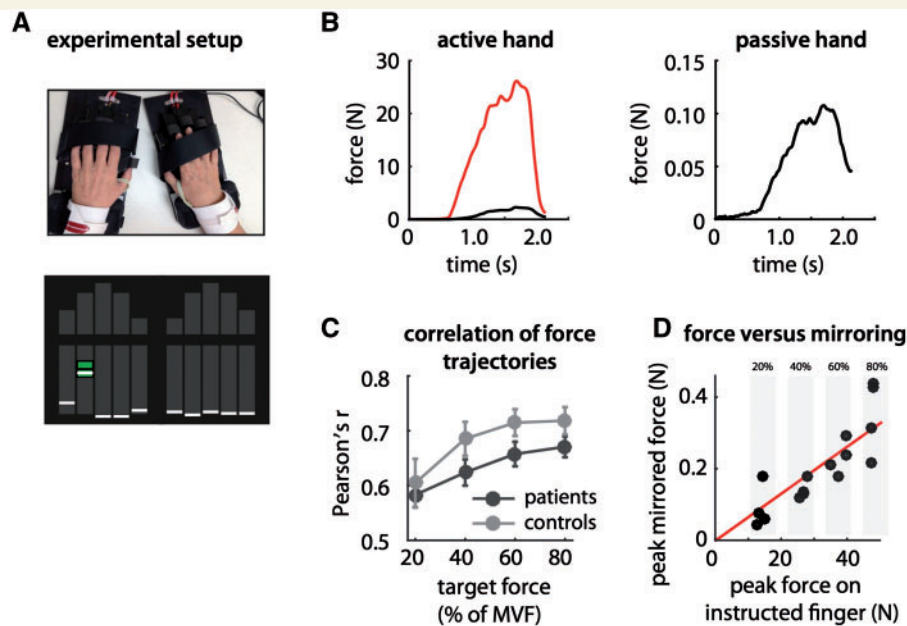


Figure 1 Assessment of mirror movements. (A) Both hands were strapped onto an ergonomic hand device capable of measuring isometric forces generated at the fingertips. Controls and patients were instructed to generate isometric forces by making individuated presses to bring the cursor (short white horizontal bars) into the target zone shown in green. During each measurement session, individuated finger presses were made at 20%, 40%, 60% and 80% of the maximum voluntary force (MVF) on that finger. (B) Sample of force traces produced in active and passive hand. Force presses with the instructed finger (thumb in right hand shown in red) resulted in involuntary forces on the passive fingers of the same hand (black), and subtle mirrored forces on the fingers of the passive hand (right). (C) Mirrored force trajectories were similar to that for the instructed finger, especially at higher target force levels. (D) Mirroring was quantified as the linear slope between the peak forces produced by the instructed finger and the peak averaged forces on the passive hand. The linear slope was log-transformed to allow the use of parametric statistical test, but for the purpose of clarity the raw values of the linear slope are reported in all subsequent figures.

Table 1 Patient information and measurement schedules for the behavioural and functional MRI experiments

| Week | 2 | 4 | 12 | 24 | 52 |
|-----------------------------------|---------------------------------|------------|-------------|--------------|-------------|
| Days (mean \pm SD) | 10 \pm 4 | 37 \pm 8 | 95 \pm 10 | 187 \pm 12 | 370 \pm 9 |
| Behavioural experiment | 53 patients, 14 controls | | | | |
| Measured at week (%) | | | | | |
| Controls | 14 (100) | 10 (71) | 12 (86) | 12 (86) | 12 (86) |
| Patients | 39 (74) | 39 (74) | 40 (75) | 39 (74) | 31 (58) |
| Fugl-Meyer (0.25–0.75 percentile) | (16–59) | (34–64) | (52–66) | (57–66) | (59–66) |
| Functional MRI experiment | 35 patients, 12 controls | | | | |
| Measured at week (%) | | | | | |
| Controls | 11 (92) | 10 (83) | 11 (92) | 11 (92) | 11 (92) |
| Patients | 24 (69) | 31 (89) | 27 (77) | 28 (80) | 19 (54) |
| Fugl-Meyer (0.25–0.75 percentile) | (16–60) | (45–65) | (59–65) | (60–66) | (64–66) |

A total of 53 patients and 14 age-matched controls were recruited for the study and measured at five different time points over the course of a year. For the behavioural experiment, each participant in the study was on average measured over at least three sessions (patients, 3.5 ± 1.5 sessions; controls, 4.3 ± 1.4), with the overall experimental data being 70.1% complete for patients and 85.7% complete for controls. For the functional MRI experiment, a subset of participants from the cohort were measured ($n = 12$ controls and $n = 35$ patients), with the experimental data being 73.7% complete for patients and 90% for controls.

(Fig. 1B). These mirrored forces were substantially smaller than the forces produced by the instructed finger. Even at the lowest target-force levels, the trajectory of these averaged mirrored forces correlated strongly with those produced by the instructed fingers (Fig. 1C). This was true for both controls [$r = 0.63$, 95% confidence interval (CI): 0.53–0.72], and patients ($r = 0.61$, 95% CI: 0.56–0.65). These correlations increased monotonically as the target-forces increased, consistent with previous reports that mirrored forces are a function of the force applied with the active hand (Todour and Lazarus, 1986; Armatas et al., 1996).

To quantify peak forces produced during mirroring, the resting baseline force on each finger prior to movement was subtracted from the subsequent force trace produced during the trial. Then the peak force $F_{passive}$ on the passive hand was calculated as the peak averaged force on the fingers during the trial:

$$F_{passive} = \max_t \left(\frac{\sum_{p=1}^5 |\tilde{F}(t, p)|}{5} \right) \quad (1)$$

where t is the duration of the trial in seconds, and \tilde{F} are the baseline corrected forces on finger p of the passive hand. Thus, $F_{passive}$ indicates the peak averaged force in the passive hand when the active finger produces force.

The passive mirrored force increased approximately linearly with the force exerted by the active hand (Fig. 1D). To derive a singular metric of the degree of mirroring across the different target force levels, we conducted a regression analysis to estimate the ratio of the peak force on the instructed finger F_{active} and the peak mirrored force ($F_{passive}$). First, all trials belonging to movements of the same instructed finger were grouped together. We plotted F_{active} on the x -axis and $F_{passive}$ for corresponding trials on the y -axis and estimated the best-fit line forced through the origin that described the data points (Fig. 1D). Sensitivity to outliers was reduced by using robust regression with a b-squared weighting function. To ensure that the passive force was specific to mirroring and not due to spurious finger presses of the passive hand, we only used trials where the correlations between averaged force trajectories across all fingers in the active and passive hands were ≥ 0.2 to estimate the linear slope.

Finally, to allow for the use of parametric statistics, the regression slope (i.e. the estimate of the ratio) was log-transformed to make it conform better to a normal distribution. This log-slope provides a sensitive measure of mirroring in the passive hand due to movements of the instructed finger. For each participant, the log-slopes associated with the instructed fingers on each hand were averaged to get a composite metric of the degree of mirroring.

Quantifying recruitment of fingers during mirror movements

The principal aim of this study was to determine how fingers of the passive hand were recruited during mirroring. To do so, we first calculated the mirroring across all 25 possible combinations of instructed/non-instructed finger pairs. Mirroring across each finger pair (i, j) was computed as described in the preceding section, by computing the log-slope between the peak force in the instructed finger i , and the peak force on the non-instructed finger j . The pattern of finger recruitment during mirroring was quantified separately for each participant and measurement session, thereafter referred to as ‘mirroring pattern’.

To determine the degree of homologous mirroring, we averaged the log-slopes for homologous finger pairs ($i = j$) across the two hands for each participant. Non-homologous mirroring was determined by averaging log-slopes for all finger pairs where $i \neq j$.

Estimating changes in mirroring patterns over time

To estimate similarities between mirroring patterns for patients and controls, we first estimated the average mirroring pattern for all controls. This control pattern was then correlated with the corresponding mirroring pattern for each patient, separately for each week. The resulting correlations quantified the similarities between mirroring patterns for patients and controls during recovery. Since the mirroring patterns for controls were themselves estimated in the presence of measurement noise, even a perfect match between patient and control

mirroring patterns would not result in a correlation of 1. To estimate a noise ceiling for the correlations, we calculated the average correlation of each controls' mirroring pattern with the group mean. As a lower bound, each control's mirroring pattern was also correlated with the group mean in which this participant was removed. These upper and lower bounds therefore specify the range of values correlations between mirroring patterns for control and patients could maximally take given measurement noise.

Quantifying finger individuation ability

In addition to the mirrored forces, individuated finger presses also resulted in enslaved forces on the uninstructed fingers of the active hand (Fig. 1B). These enslaved forces were generally much larger than the associated mirrored forces, and at high force requirements, degraded the participants ability to individuate a single finger (Li *et al.*, 1998). We quantified the degree of enslaving in the same way as for mirroring, by estimating the log-slope between the peak forces on the instructed and the passive fingers on the active hand, respectively. We have previously used a similar metric to quantify patients' impairment in finger individuation ability after stroke (Xu *et al.*, 2017).

Assessing neural activity associated with individuated finger movements using functional MRI

Cortical activity associated with finger movements was measured in controls and patients at the same time points as for the behavioural measurements, five times over the course of a 1-year period (Table 1).

Participants were instructed to produce individuated finger movements inside an MRI scanner in a protocol resembling the behavioural task. To reduce scanning time, only four fingers on either hand were tested (ring finger was excluded). Each trial required the production of four short isometric force presses with an instructed finger. Each trial began with the instructed finger highlighted in green for 2 s. A green line then appeared below the finger stimulus as the go-cue for producing a short flexion force press with the instructed finger within 1.9 s. This cue was repeated four times for a total of four repetitive presses with the instructed finger for that trial. A successful finger press required the production of either 1.8 N or 8% of the maximum voluntary force for that finger, whichever was lower. The green line turned blue to signal a successful finger press. Trials were grouped as experimental runs, with each run consisting of three trials for the eight fingers across the two hands (a total of $3 \times 8 = 24$ trials/run). Trials within each run were presented in pseudo-random order, and participants performed eight runs at each measurement session.

Functional scans during task performance were obtained at three centres on two different 3T Philips systems (Achieva and Ingenia). Scans were obtained with a 32-channel head-coil using a two-dimensional echo-planar imaging sequence (repetition time = 2 s, 35 slices, 154 volumes per run, slice thickness 2.5 mm, 0 mm gap, in-plane resolution 2.5×2.5 mm²). Scans obtained in Zurich had 31 slices but were otherwise identical. Within each imaging run, six rest phases lasting 10 s were

randomly interspersed. A T₁-weighted anatomical image (3D MPRAGE sequence, $1 \times 1 \times 1.2$ mm, $256 \times 256 \times 170$ mm field of view) was also acquired. For each participant, two diffusion tensor-imaging (DTI) images (repetition time = 6.6 s, 60 slices, 2.2 mm slice thickness, 212×212 mm field of view) were also acquired to help quantify the size and location of stroke lesions.

Imaging analysis

All functional data were corrected for motion across runs (Diedrichsen and Shadmehr, 2005), and co-registered to the T₁ image obtained in the participant's first measurement session (either Week 2 or 4). The raw time-series data were analysed using a generalized-linear model (GLM) with a separate regressor for each finger/hand/imaging run (four fingers \times two hands \times eight runs = 64 regressors). Activation for each trial was modelled using a boxcar function (10.88 s) convolved with a standard haemodynamic response function.

Each participants T₁ image was used to reconstruct the pial and white-grey matter surfaces using Freesurfer (Dale *et al.*, 1999). Individual surfaces were aligned across participants and registered to match a template using the sulcal-depth map and local curvature as minimization constraints.

The anatomical regions of interest were defined on the group surface using probabilistic cyto-architectonic maps aligned to the average surface (Fischl *et al.*, 2008). Surface nodes with the highest probability for Brodmann area (BA4) 2 cm above and below the hand-knob were selected as belonging to M1 (primary motor cortex). Similarly, nodes in the hand-region in S1 (primary somatosensory cortex) were isolated using BA 3a, 3b, 1 and 2 (combined), again 2 cm above and below the hand knob.

Each participants DTI and T₁ images (at first measurement) were used to estimate the size and location of lesions in two regions of interest: (i) cortical grey matter in the sensorimotor cortices (M1/S1) of either hemisphere; and (ii) the corticospinal tract superior to the pyramids. Lesion boundaries were determined independently by radiologist (A.V.F.) and neurologist (M.B.) that were blind to the patients' clinical information and task performance. Detailed information about lesion distribution can be found in Xu *et al.* (2017).

Finally, the parameter estimates from the GLM analysis in M1 and S1 regions of interest with lesion areas excluded, were identified and pre-whitened using the GLM residuals to reduce the effects of estimation noise (Walther *et al.*, 2015). These pre-whitened parameter estimates quantified the evoked blood oxygen level-dependent (BOLD) activations.

Statistical analysis and missing data

As measuring participant data for all five sessions was ambitious, we ended up with an unbalanced experimental design due to missing data across both the behavioural and the functional MRI experiments. The percentages of successfully measured sessions for behavioural and imaging experiments are reported in Table 1.

To deal with the incomplete and unbalanced data in a statistically efficient way, we used a linear mixed-effects model with time-point/conditions as fixed effects and participant as a random effect. The mixed-effects model was estimated using the *lme4* package in R (Bates *et al.*, 2014). Mean estimates (and confidence intervals) were used to provide summary plots

(Fig. 3D), and we used χ^2 tests to assess the significance of the fixed effects or their interactions. The use of the mixed-model efficiently solves the missing data problem with using data interpolation (which can induce biases) or data imputation (which is statistically inefficient). All data presented in the text and figures are represented as mean \pm standard error of the mean (SEM). All statistical tests involving correlations were performed on Fisher Z-transformed values.

Results

Mirror movements appeared early after stroke and normalized over the year

Using a sensitive behavioural assay, we quantified mirror movements in 53 stroke patients and 14 controls. Patients showed large time course changes in mirroring in the year following a stroke (Fig. 2A). In the first 2 weeks after damage (Week 2), individuated finger presses with the paretic hand resulted in large forces in the non-paretic hand, with 1 N of voluntary force resulting in ~ 0.051 N of averaged mirrored force. In comparison, mirroring in controls was significantly lower than patients [0.004 N/1 N; $t(51) = 3.67$, $P = 0.001$]. Mirroring in patients subsequently reduced over time ($\chi^2 = 82.99$, $P \ll 0.0001$). However, even 6 months after stroke, mirroring was still marginally larger in comparison to controls [0.007 N/1 N; $t(51) = 1.75$, $P = 0.087$]. There was a strong correlation between mirroring during the early and late stages following stroke $r = 0.73$ ($P < 0.001$), demonstrating that patients who exhibited large mirroring early after stroke continued to do so throughout recovery.

The longitudinal changes in mirroring were remarkably similar to those for the deficits in fine-finger function in the paretic hand (Fig. 2B). After stroke, patients' efforts to produce isometric forces with a single finger resulted in

abnormally large forces in the uninstructed fingers of the paretic hand. These enslaved forces signify the loss of fine-finger control in patients (Li et al., 2003; Xu et al., 2017). Early after damage (Week 2), enslaving in patients was significantly larger than controls, demonstrating a substantial loss of individuated finger control [controls 0.042 N/1 N; patients 0.170 N/1 N; $t(51) = 4.02$, $P < 0.001$]. Enslaving progressively reduced over the course of the year ($\chi^2 = 28.38$, $P \ll 0.0001$), but never fully normalized even by 6 months post-stroke [$t(51) = 3.09$, $P = 0.003$]. Patients who had large enslaving early after stroke also demonstrated large mirroring at the same time-period (enslaving and mirroring at Week 2, $r = 0.78$, $P \ll 0.0001$), and continued to do so even by the chronic stage of recovery (enslaving Week 2 and mirroring Week ≥ 24 , $r = 0.66$, $P = 0.0001$).

We also quantified the degree of mirror movements in the paretic hand during non-paretic finger presses. Early after damage (Week 2), mirror movements in the paretic hand were slightly reduced in comparison to controls [Week 2; 0.002/1 N; $t(50) = 1.61$, $P = 0.114$]. Paretic mirroring became progressively larger as patients recovered ($\chi^2 = 10.82$, $P = 0.029$).

Consistent with earlier findings, here we report that mirroring in the non-paretic hand was exaggerated after stroke (Nelles et al., 1998; Wittenberg et al., 2000; Kim et al., 2003), and slightly reduced in the paretic hand (Nelles et al., 1998). We further report that non-paretic mirroring appeared with a time course that paralleled that for the fine-control deficits in the paretic hand.

No modulation of evoked BOLD activities in the bilateral sensorimotor cortices after stroke

Next, we considered whether increased recruitment of the sensorimotor cortex in non-lesioned hemisphere could

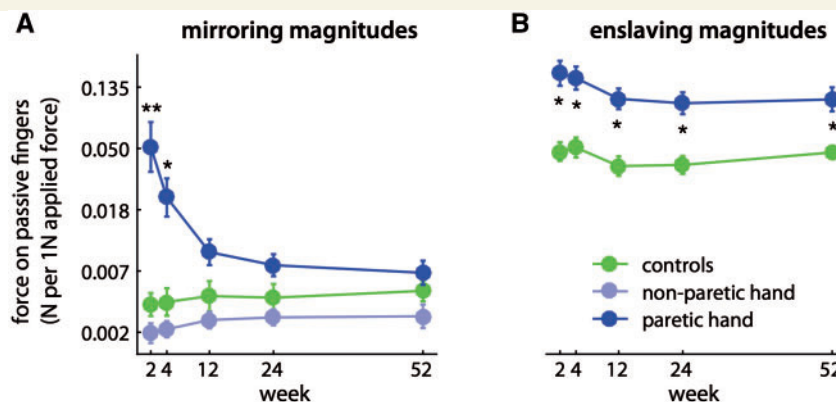


Figure 2 Longitudinal changes in mirror movements and fine-finger control after stroke. (A) Changes in mirroring for controls and patients measured in the first year after stroke. Line plots are labelled by the active hand. For patients, mirroring was primarily measured in the fingers of the non-paretic hand, during active finger presses with the paretic hand. Mirroring in the paretic hand during non-paretic finger presses is also shown. (B) Associated changes in fine-finger control on the active hand across groups. Individuated finger presses in patients and controls resulted in undesired force contractions on the uninstructed fingers of the active hand. The larger these so-called enslaved movements, the worse the degree of fine-finger control. For clarity, the raw values of the linear-slope estimates for mirroring and enslaving are plotted in A and B. Group differences within each week are indicated by $**P < 0.001$ and $*P < 0.01$.

explain the time course of exaggerated mirror movements in the non-paretic hand. If mirroring is indeed caused by overactivation of the non-lesioned sensorimotor cortex, then the time course of these activations should resemble the time course changes in mirroring quantified earlier (Fig. 2A). To test this idea, we used functional MRI to measure evoked activities in the hand area of S1/M1, in a smaller subset of participants from the same study cohort (Table 1; 35 patients, 12 controls). Participants performed individuated finger presses inside an MRI scanner (Fig. 3A). During paretic finger presses, patients demonstrated the same mirroring and enslaving behaviour both inside and outside the scanner environments (Fig. 3B and C; mirroring, $r = 0.89$, $P \ll 0.001$; enslaving, $r = 0.75$, $P \ll 0.001$).

The resulting evoked BOLD responses in S1/M1 for patients were remarkably stable throughout recovery (Fig. 3D; statistics in Table 2). For paretic hand presses, patients demonstrated the stereotypical pattern of evoked cortical responses seen for unimanual finger presses in healthy controls, which was characterized by an increase and reduction of BOLD responses in the contra- and ipsilateral sensorimotor cortices, respectively. There were no time course-related changes in evoked activities in either

the contra- or the ipsi-lateral cortices, with activations in either hemisphere indistinguishable from the control group. In the post-stroke period, no consistent relationship was found between mirror movements in the non-paretic hand and activities in the contra- and ipsilateral sensorimotor cortices (Supplementary Table 1).

To summarize results from our first analysis, we report that the clear occurrence of the longitudinal changes in mirroring after stroke were not accompanied by overactivations in the sensorimotor cortices of either the non-lesioned or the lesioned hemispheres.

Mirror movements were characterized by the recruitment of multiple fingers

Next, we were interested in understanding the pattern with which fingers in the non-paretic hand were recruited during mirroring. Specifically, we wanted to determine whether mirroring appeared primarily in the homologous fingers (indicating a cortical locus, see Introduction), or whether fingers in the non-paretic hand were recruited broadly

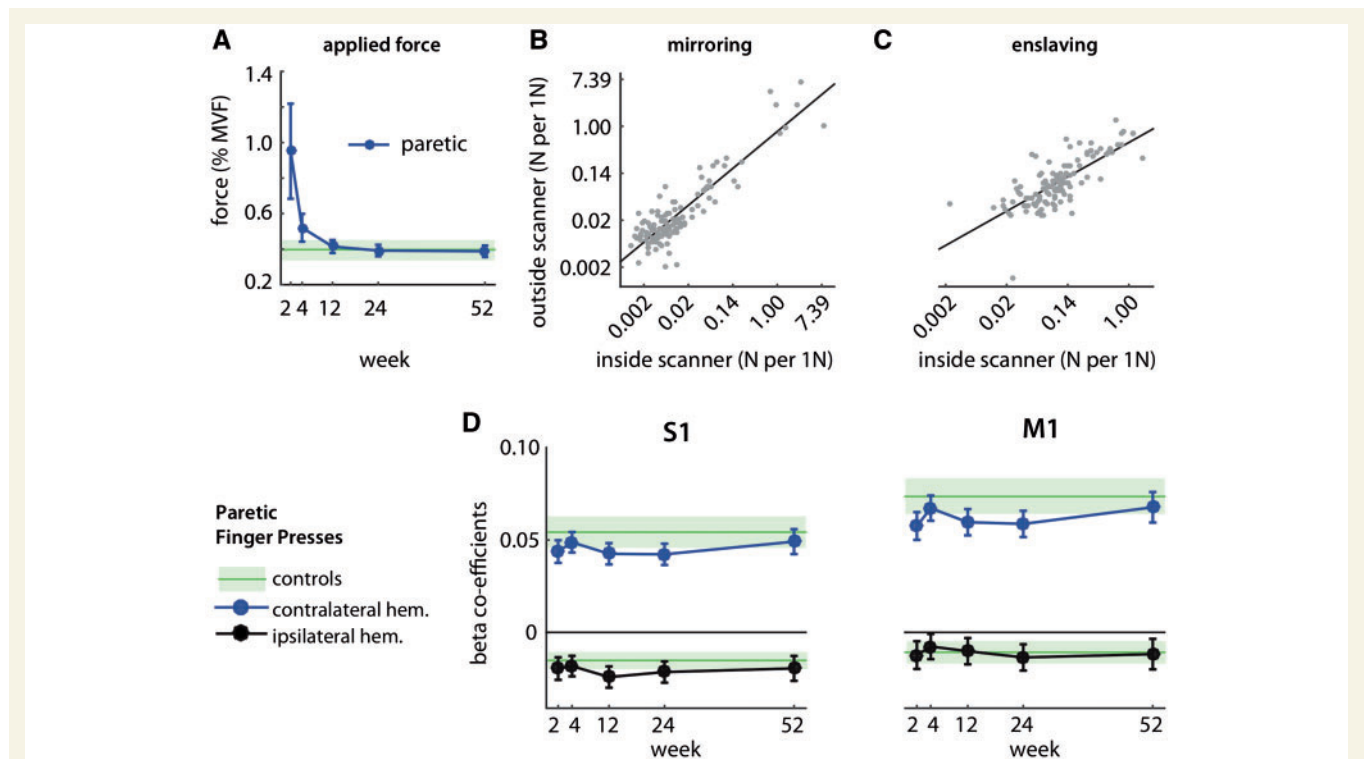


Figure 3 Evoked BOLD activities for finger presses in the primary somatosensory (S1) and motor (M1) cortices. (A) During the functional MRI task, patients and controls were required to produce either 1.8 N or 8% of the maximum voluntary force (MVF) on the instructed finger. Forces are expressed as a percentage of maximum voluntary force. Controls produced forces at $\sim 40\%$ of maximum voluntary force. From Week 4 onwards, forces produced by patients and controls were not significantly different (Week ≥ 4 ; $\chi^2 = 0.02$, $P = 0.887$). (B) Measurements of mirroring on the non-paretic hand were highly correlated inside and outside the scanner environments. (C) Similarly, enslaving in the paretic hand was highly correlated for measurements inside and outside the scanner environments. Each dot in B and C represents the session measurement of a single patient. For clarity, the raw values of the linear-slope estimates for mirroring are plotted in B and C. (D) Evoked BOLD activities in contra- and ipsilateral S1 and M1 cortices due to paretic finger presses. Corresponding contra and ipsilateral activities in controls are depicted by the shaded green regions (mean \pm SEM).

Table 2 Statistics for the functional MRI experiment

| | Change over weeks | | Similarity with controls | |
|------------------------------|-------------------|----------|--------------------------|----------|
| | χ^2 | <i>P</i> | χ^2 | <i>P</i> |
| Activity for paretic presses | | | | |
| Contralateral (S1) | 1.410 | 0.842 | 1.160 | 0.282 |
| Contralateral (M1) | 2.070 | 0.723 | 1.150 | 0.285 |
| Ipsilateral (S1) | 1.860 | 0.761 | 0.813 | 0.367 |
| Ipsilateral (M1) | 1.250 | 0.870 | 0.010 | 0.915 |

Statistics are shown for differences in contralateral and ipsilateral M1/S1 activations, across weeks (first two columns) and between patients and controls (last two columns).

(favouring a subcortical locus). We therefore characterized mirroring patterns across all active/passive fingers in both controls and patients (see ‘Materials and methods’ section).

The degree of mirroring in each passive finger as a function of the instructed finger can be seen in Fig. 4A. The overall patterns of mirroring across all active/passive finger pairs themselves were highly reliable, with split-half correlations being $r > 0.85$ for both controls and patients (Supplementary Table 2). The first immediate observation is that mirroring was not restricted to the homologous fingers (diagonal), but that substantial effects could also be observed on non-homologous fingers (off-diagonal). To quantify this observation, we partitioned mirroring across the different active/passive finger pairs into their respective homologous and non-homologous components (see ‘Materials and methods’ section).

In controls, finger presses resulted in a broad recruitment of fingers in the passive hand. Finger presses in the active hand were highly individuated in nature, with 1 N of force on the instructed finger resulting in 0.042 N of enslaved forces (ratio of 24.77 ± 2.18 ; Fig. 2B). These finger presses resulted in mirroring across both homologous and non-homologous fingers pairs. While homologous mirroring was, on average, larger than the non-homologous component [$t(13) = 5.421$, $P = 0.0001$], some finger presses resulted in nearly equivalent effects on both [index finger presses; $t(13) = 1.23$, $P = 0.240$, ring; $t(13) = 0.88$, $P = 0.398$]. Overall, forces in the passive hand were much more evenly distributed across fingers than the forces in the active hand (Fig. 4B), with the corresponding ratio between homologous and non-homologous mirroring components (1.61 ± 0.16) being nearly 15 times smaller than the instructed/enlaving ratio on the active hand [$t(13) = 28.26$, $P \ll 0.0001$]. Thus, mirroring was not simply due to a symmetric digit-by-digit activation of the motor system, as predicted from the exact mirroring of cortical activity patterns across hemispheres (Scherer et al., 2009; Liu et al., 2010; Diedrichsen et al., 2013).

Similarly, in patients, finger presses with the paretic hand resulted in a broad recruitment of fingers in the non-parietic hand. The year-long changes in mirroring characterized earlier (Fig. 2A) were observed in both homologous and non-homologous fingers (Fig. 4C; change over weeks: homologous, $\chi^2 = 71.35$, $P \ll 0.0001$, non-homologous, $\chi^2 = 78.15$, $P \ll 0.0001$), with homologous mirroring

being the stronger of the two ($\chi^2 = 24.53$, $P \ll 0.0001$). Critically, despite these longitudinal changes, the ratio between homologous and non-homologous mirroring (1.76 ± 0.12) remained stable across weeks ($\chi^2 = 1.16$, $P = 0.885$) and was at the same level as healthy controls ($\chi^2 = 0.10$, $P = 0.754$). Remarkably, when considering mirroring across all active/passive fingers irrespective of the homologous and non-homologous finger (Fig. 5), a high degree of similarity between finger recruitment patterns for patients and controls was observed. Throughout recovery, mirroring patterns for patients looked like a scaled version of the corresponding control mirroring pattern.

To summarize, finger presses in patients, like controls, broadly recruited fingers in the passive hand. Throughout recovery, mirroring patterns for patients looked remarkably similar to scaled versions of the control pattern. The most parsimonious explanation for this similarity is that a single system is responsible for mirroring in controls, and it is up-regulated in the non-parietic hand after stroke.

Discussion

In this study, we characterized mirror movements in the non-parietic hand in 53 patients in the year following stroke. We have provided the first comprehensive characterization of the time course, as well as the pattern with which fingers in the non-parietic hand were recruited during individuated paretic finger presses.

Consistent with earlier findings, we found that mirroring was exaggerated in the non-parietic hand post-stroke (Nelles et al., 1998; Wittenberg et al., 2000; Kim et al., 2003; Sehm et al., 2009). We expanded upon these previous studies by showing that mirroring appeared early after stroke and diminished as the hand recovered function. Despite these time course changes in mirroring, we did not find any overactivations in the sensorimotor cortices in either hemisphere. These sensorimotor areas (M1/S1) provide the bulk of the inputs to the corticospinal pathways that provide fine-finger control (Lemon, 2008; Porter and Lemon, 1993; Lemon, 2008), and the lack of evoked BOLD modulation in these areas suggests that a simple up/down regulation of overall activity is unlikely to be the mechanism of mirroring after stroke. Although we cannot completely rule out that BOLD responses might

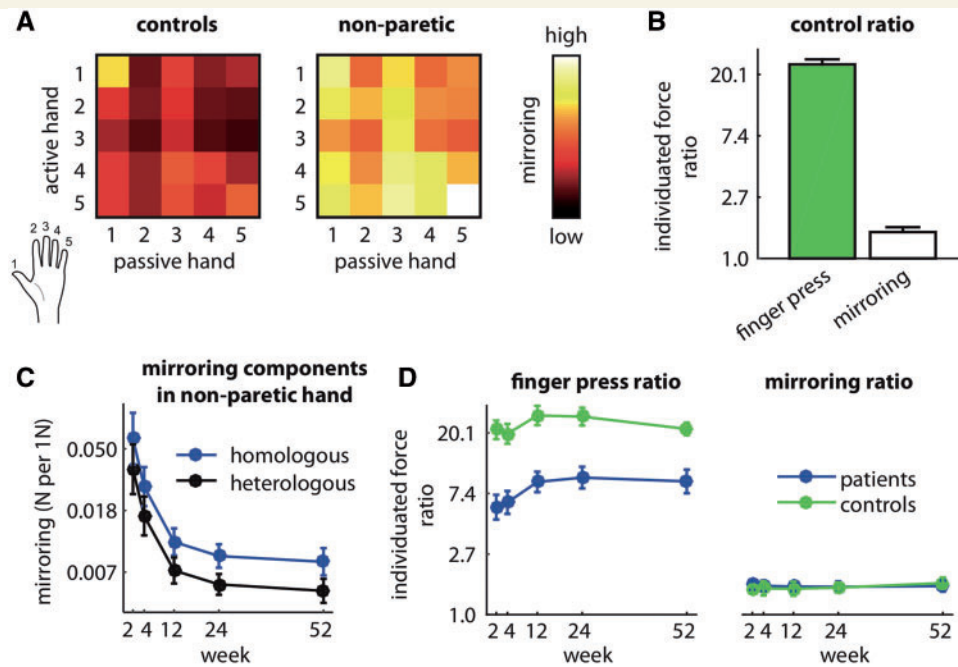


Figure 4 Relative contributions of homologous and non-homologous components to mirror movements on the non-paretic hand. (A) Mirroring across all possible active/passive finger pairs for controls and patients (on non-paretic hand only). Rows and columns denote which finger was pressed on the active hand, and the finger on the passive hand that mirroring was estimated on, respectively. Diagonal and off-diagonal matrix entries represent mirroring across homologous and non-homologous finger pairs. (B) Individualized finger presses by controls resulted in enslaved forces on the passive fingers of the same hand and mirrored forces across homologous and non-homologous finger pairs. The ratio between instructed/enslaved forces within the active hand is shown in green, while the ratio between homologous and non-homologous mirroring components is shown in white. Shown here are data for controls averaged across all five measurement sessions. (C) Changes in homologous and non-homologous mirroring components on the non-paretic hand in the year following stroke. For clarity, the raw values of the linear-slope estimates for mirroring are plotted. (D) For patients, the ratios between instructed/enslaved forces on the paretic hand, and the ratio between homologous/non-homologous mirroring patterns are shown in the left and right panels, respectively.

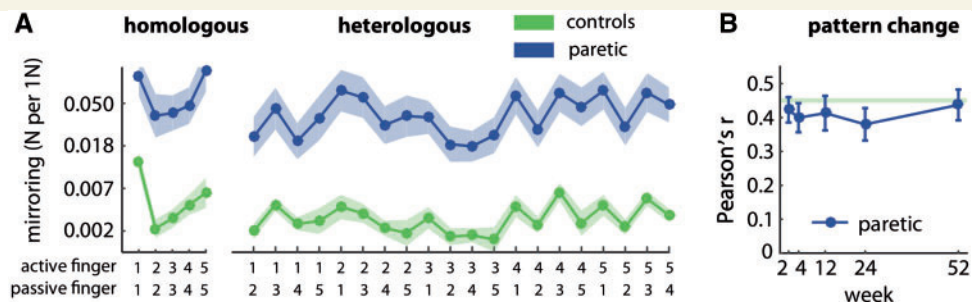


Figure 5 Stability of mirroring pattern during stroke recovery. (A) The average mirroring patterns across all active/passive finger pairs are shown for patients (Week 2) and controls. For clarity, the raw values of the linear-slope estimates for mirroring are plotted in A. Similarity between the patterns for patients and controls was high, even in the early period after stroke (Week 2, $r = 0.88$, $P \ll 0.0001$). (B) Correlations between mirroring patterns for patients and controls remained unchanged throughout recovery ($\chi^2 = 1.87$, $P = 0.760$). The pattern correlations for patients and controls were also close to noise ceilings; i.e. the maximum possible pattern correlations possible given the measurement noise on mirroring patterns for each control (see 'Materials and methods' section).

have been insensitive to subtle changes in sensorimotor activity required to produce the small forces during mirroring, our results contradict earlier studies that have argued that exaggerated non-paretic mirroring is caused by over-activations in ipsi- or contralesional M1/S1 (Wittenberg *et al.*, 2000; Kim *et al.*, 2003; Cincotta and Ziemann, 2008). These results question the validity of trans-callosal

model of stroke recovery (Di Pino *et al.*, 2014) as an explanation for mirror movements in the non-paretic hand. Rather, the lack of activity modulation in either the lesioned and non-lesioned sensorimotor cortices hints at a subcortical origin for these mirror movements.

Additional evidence for a subcortical locus comes from our inspection of the exact pattern of mirrored forces in the

non-paretic hand. We quantified the distribution of mirrored forces across homologous and/or non-homologous fingers. We argue that cortical contributions to mirroring would manifest themselves primarily in the homologous fingers. This prediction is based on recent functional MRI studies that show that the activity patterns in sensory-motor cortices during ipsilateral movements are highly correlated with those evoked by contralateral movements (Diedrichsen *et al.*, 2013). Indeed, these ipsilateral patterns can be completely modelled as scaled-down versions of the activity patterns for the mirror-symmetric finger (Diedrichsen *et al.*, 2017). We therefore would expect that the mirroring generated cortically would be a scaled down, but otherwise identical version of the force pattern generated in the active hand.

In contrast, mirror movements generated through subcortical pathways should result in very different forces across fingers of the non-paretic hand. Subcortical pathways such as the reticulospinal system can only support limited finger individuation (Lawrence and Kuypers, 1968b; Soteropoulos *et al.*, 2012), and would hence lead to a broad distribution of mirrored forces across non-paretic fingers. Two results from this study point towards a subcortical origin of mirror movements. First, we found that non-paretic fingers were broadly recruited during mirroring, with the ratio of forces between homologous and non-homologous fingers being ~ 1.7 , much lower than what would be expected from ratio of active/enforced forces in the paretic hand (~ 7.4). Second, the mirroring pattern across all active/passive fingers looked remarkably similar for patients and controls, with the patient pattern resembling a scaled version of the control pattern, suggesting that the system that is responsible for mirroring in controls is upregulated after stroke. It is worth pointing out that part of this similarity could be due to similar musculo-skeletal features of the hand across individuals. Nevertheless, the most parsimonious explanation is that mirror movements are caused by a subcortical system with limited individuation capability that is upregulated after stroke.

One candidate subcortical pathway for mirror movements is the reticulospinal system (Lawrence and Kuypers, 1968b; Riddle *et al.*, 2009; Baker, 2011; Soteropoulos *et al.*, 2012; Zaami *et al.*, 2012). The reticulospinal system provides input to both proximal and distal muscles of the upper limb (Riddle *et al.*, 2009; Baker, 2011; Soteropoulos *et al.*, 2012) and could therefore contribute to the control of finger movements. One piece of supportive evidence for the role of the reticulospinal system in mirroring comes from comparing the patterns of upper limb muscle recruitment during mirroring in humans, with muscle responses measured following stimulation of subcortical pathways in primates. For instance, in young children, flexion of the elbow joint results in mirroring mostly on the extensor muscles of the opposing elbow (Missiuro, 1963). This recruitment of ipsilateral flexors and contralateral extensor shoulder muscles is a prominent muscle activity pattern observed during stimulation of neurons in the ponto-medullary reticular formation (Herbert *et al.*, 2010; Hirschauer and Buford, 2015).

If recovery of paretic hand function relies increasingly on the capacity of the reticulospinal system to compensate for cortical damage (Xu *et al.*, 2017), and if the reticulospinal system is responsible for contributing towards mirror movements, then how does mirroring reduce over the same time while paretic hand function recovers? One possible answer to this puzzle could be that reduction of non-paretic mirroring and paretic hand recovery both rely on the ability of spared corticospinal (McNeal *et al.*, 2010) and cortico-subcortical connections (Herbert *et al.*, 2015) to regain control over the reticulospinal system. It's very likely that the reticulospinal system is activated during hand use even in healthy individuals, especially during grasping, but that its overall expression is modulated by cortical sensorimotor areas through cortico-subcortical connections. This shared cortico-subcortical control of hand function would predict that the reticulospinal system activates preferentially during grasping where the production of high-force levels is required, but remains relatively silent during the production of fine-individuated movements. A loss of cortical input might therefore up regulate contributions from the reticulospinal system post-stroke leading to compensatory control of the paretic but exaggerated mirroring in the non-paretic hands, respectively. During the course of recovery, a reduction in both enslaving and mirroring would then be reliant on the capacity of sensorimotor areas in the lesioned and non-lesioned hemispheres to re-establish a modulatory influence on the reticulospinal tract.

In conclusion, we have provided a detailed characterization of both the time course and pattern of mirror movements following stroke. Our results suggest that interactions between cortical and subcortical motor areas are critical to hand recovery after stroke. Our study raises the exciting possibility that mirror movements can offer a window through which these interactions can be studied.

Web resources

Behavioural dataset available at: <https://github.com/nejaz1/mirroring2017>

Preprint posted on bioRxiv.

Acknowledgements

We would like to thank the tireless work of the many therapists and research associates that helped in the different facets of this project. We would also like to thank the patients for their valuable time and effort.

Funding

The main study was supported by a James S. McDonnell Foundation award (JMSF 220020220) to J.W.K. Additional support came from a Scholar Award from the James S. McDonnell Foundation and a Grant from the

Wellcome Trust (094874/Z/10/Z) to J.D. A.R.L. is supported by the P&K Pühringer Foundation. P.A.C. is supported by an NIH R01 grant (5R01HD053793).

Supplementary material

Supplementary material is available at *Brain* online.

References

- Armatas CA, Summers JJ, Bradshaw JL. Handedness and performance variability as factors influencing mirror movement occurrence. *J Clin Exp Neuropsychol* 1996; 18: 823–35.
- Baker SN. The primate reticulospinal tract, hand function and functional recovery. *J Physiol* 2011; 589: 5603–12.
- Bates D, Mächler M, Bolker B, Walker S. Fitting linear mixed-effects models using lme4. *arXiv preprint arXiv:1406.5823*. 2014.
- Cernacek J. Contralateral motor irradiation-cerebral dominance: its changes in hemiparesis. *Arch Neurol* 1961; 4: 165–72.
- Cincotta M, Ziemann U. Neurophysiology of unimanual motor control and mirror movements. *Clin Neurophysiol* 2008; 119: 744–62.
- Cramer SC, Nelles G, Benson RR, Kaplan JD, Parker RA, Kwong KK, et al. A functional MRI study of subjects recovered from hemiparetic stroke. *Stroke* 1997; 28: 2518–27.
- Dale AM, Fischl B, Sereno MI. Cortical surface-based analysis: I. Segmentation and surface reconstruction. *Neuroimage* 1999; 9: 179–94.
- Di Pino G, Pellegrino G, Assenza G, Capone F, Ferreri F, Formica D, et al. Modulation of brain plasticity in stroke: a novel model for neurorehabilitation. *Nat Rev Neurol* 2014; 10: 597–608.
- Diedrichsen J, Shadmehr R. Detecting and adjusting for artifacts in fMRI time series data. *Neuroimage* 2005; 27: 624–34.
- Diedrichsen J, Wiestler T, Krakauer JW. Two distinct ipsilateral cortical representations for individuated finger movements. *Cereb Cortex* 2013; 23: 1362–77.
- Diedrichsen J, Yokoi A, Ar buckle SA. Pattern component modeling: A flexible approach for understanding the representational structure of brain activity patterns. *NeuroImage* 2017, Advance Access published on August 24, 2017, doi: 10.1016/j.neuroimage.2017.08.051.
- Ejaz N, Hamada M, Diedrichsen J. Hand use predicts the structure of representations in sensorimotor cortex. *Nat Neurosci* 2015; 18: 1034–40.
- Fischl B, Rajendran N, Busa E, Augustinack J. Cortical folding patterns and predicting cytoarchitecture. *Cerebral* 2008; 18: 1973–80.
- Goodglass H, Quadfasel FA. Language laterality in left-handed aphasics. *Brain* 1954; 77: 421–8.
- Herbert WJ, Davidson AG, Buford JA. Measuring the motor output of the pontomedullary reticular formation in the monkey: do stimulus-triggered averaging and stimulus trains produce comparable results in the upper limbs? *Exp Brain Res* 2010; 203: 271–83.
- Herbert WJ, Powell K, Buford JA. Evidence for a role of the reticulospinal system in recovery of skilled reaching after cortical stroke: initial results from a model of ischemic cortical injury. *Exp Brain Res* 2015; 233: 3231–51.
- Hirschauer TJ, Buford JA. Bilateral force transients in the upper limbs evoked by single-pulse microstimulation in the pontomedullary reticular formation. *J Neurophysiol* 2015; 113: 2592–604.
- Kim Y, Kim W-S, Shim JK, Suh DW, Kim T, Yoon B. Difference of motor overflow depending on the impaired or unimpaired hand in stroke patients. *Hum Mov Sci* 2015; 39: 154–62.
- Kim YH, Jang SH, Chang Y, Byun WM, Son S, Ahn SH. Bilateral primary sensori-motor cortex activation of post-stroke mirror movements: an fMRI study. *Neuroreport* 2003; 14: 1329–32.
- Lan Y, Yao J, Dewald JPA. The impact of shoulder abduction loading on volitional hand opening and grasping in chronic hemiparetic stroke. *Neurorehabil Neural Repair* 2017; 31: 521–9.
- Lawrence DG, Kuypers HG. The functional organization of the motor system in the monkey. I. The effects of bilateral pyramidal lesions. *Brain* 1968a; 91: 1–14.
- Lawrence DG, Kuypers HG. The functional organization of the motor system in the monkey. II. The effects of lesions of the descending brain-stem pathways. *Brain* 1968b; 91: 15–36.
- Lemon RN. Descending pathways in motor control. *Annu Rev Neurosci* 2008; 31: 195–218.
- Li S, Latash ML, Yue GH, Siemionow V, Sahgal V. The effects of stroke and age on finger interaction in multi-finger force production tasks. *Clin Neurophysiol* 2003; 114: 1646–55.
- Li ZM, Latash ML, Zatsiorsky VM. Force sharing among fingers as a model of the redundancy problem. *Exp Brain Res* 1998; 119: 276–86.
- Liu Y, Sharma M, Gaona C, Breshears J. Decoding ipsilateral finger movements from ECoG signals in humans. In: *NIPS'10 Proceedings of the 23rd International Conference on Neural Information Processing Systems—Vol. 2*, 2010. Red Hook, NY: Curran Associates Inc., p. 1468–76.
- McNeal DW, Darling WG, Ge J, Stilwell-Morecraft KS, Solon KM, Hynes SM, et al. Selective long-term reorganization of the corticospinal projection from the supplementary motor cortex following recovery from lateral motor cortex injury. *J Compar Neurol* 2010; 518: 586–621.
- Missiuro W. Studies on developmental stages of children's reflex reactivity. *Child Dev* 1963; 34: 33–41.
- Nelles G, Cramer SC, Schaechter JD, Kaplan JD, Finklestein SP. Quantitative assessment of mirror movements after stroke. *Stroke* 1998; 29: 1182–87.
- Oldfield RC. The assessment and analysis of handedness: the Edinburgh inventory. *Neuropsychologia* 1971; 9: 97–113.
- Porter R, Lemon R. Corticospinal function and voluntary movement. USA: Oxford University Press, 1993.
- Riddle CN, Edgley SA, Baker SN. Direct and indirect connections with upper limb motoneurons from the primate reticulospinal tract. *J Neurosci* 2009; 29: 4993–9.
- Sakai ST, Davidson AG, Buford JA. Reticulospinal neurons in the pontomedullary reticular formation of the monkey (*Macaca fascicularis*). *Neuroscience* 2009; 163: 1158–70.
- Scherer R, Zanos SP, Miller KJ, Rao RPN, Ojemann JG. Classification of contralateral and ipsilateral finger movements for electrocorticographic brain-computer interfaces. *Neurosurg Focus* 2009; 27: E12.
- Sehm B, Perez MA, Xu B, Hidler J, Cohen LG. Functional neuroanatomy of mirroring during a unimanual force generation task. *Cereb Cortex* 2009; 20: 34–45.
- Soteropoulos DS, Williams ER, Baker SN. Cells in the monkey pontomedullary reticular formation modulate their activity with slow finger movements. *J Physiol* 2012; 590: 4011–27.
- Sukal TM, Ellis MD, Dewald JPA. Shoulder abduction-induced reductions in reaching work area following hemiparetic stroke: neuroscientific implications. *Exp Brain Res* 2007; 183: 215–23.
- Todor JI, Lazarus JAC. Exertion level and the intensity of associated movements. *Dev Med Child Neurol* 1986; 28: 205–12.
- Walther A, Nili H, Ejaz N, Alink A, Kriegeskorte N, Diedrichsen J. Reliability of dissimilarity measures for multi-voxel pattern analysis. *Neuroimage* 2015; 137: 188–200.
- Ward NS, Brown MM, Thompson AJ, Frackowiak RSJ. Neural correlates of outcome after stroke: a cross-sectional fMRI study. *Brain* 2003; 126: 1430–48.
- Wittenberg GF, Bastian AJ, Dromerick AW, Thach WT, Powers WJ. Mirror movements complicate interpretation of cerebral activation changes during recovery from subcortical infarction. *Neurorehabil Neural Repair* 2000; 14: 213–21.
- Xu J, Ejaz N, Hertler B, Branscheidt M, Widmer M, Faria AV, et al. Separable systems for recovery of finger strength and control after stroke. *J Neurophysiol* 2017; 118: 1151–63.
- Zaaimi B, Edgley SA, Soteropoulos DS, Baker SN. Changes in descending motor pathway connectivity after corticospinal tract lesion in macaque monkey. *Brain* 2012; 135: 2277–89.